Using satellite observed formaldehyde (HCHO) and nitrogen dioxide (NO_2) as an indicator of ozone sensitivity in a SIP

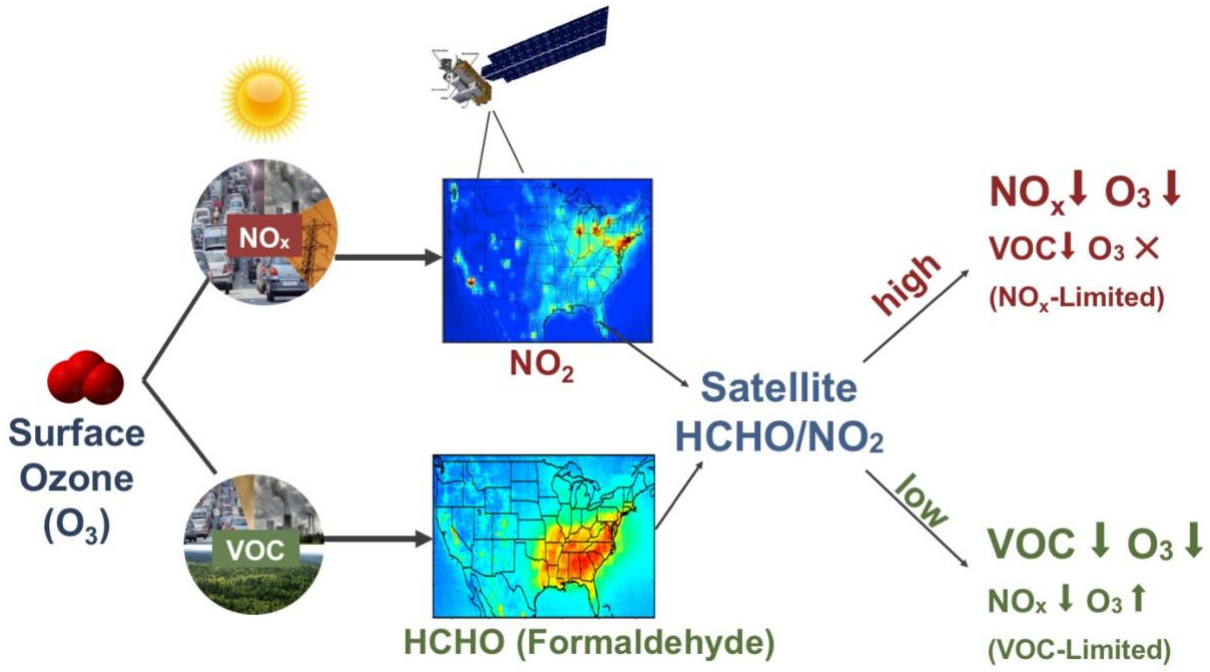

Lead Authors: Xiaomeng Jin and Arlene Fiore (LDEO/Columbia)
Michael Geigert (CT DEEP)

Document Publication Date: June 12, 2018

This technical guidance document is a product of a 2017-2018 NASA Health and Air Quality Applied Sciences Team (HAQAST; www.haqast.org) Tiger Team project, "Supporting the use of satellite data in State Implementation Plans (SIPs)". Team membership is listed below. We are grateful to colleagues who shared ideas and opinions that helped shape this document, and to NASA for hosting these products on the Air Quality From Space website at https://airquality.gsfc.nasa.gov/aq-managers.

HAQAST Tiger Team Participants

Grace Choi (gracesh27@gmail.com), University of Wisconsin—Madison
Bryan Duncan (bryan.n.duncan@nasa.gov), NASA GSFC
Arlene Fiore (amfiore@ldeo.columbia.edu), LDEO/Columbia University
Daven Henze (Daven.Henze@colorado.edu), University of Colorado – Boulder
Jeremy Hess (jjhess@uw.edu), University of Washington
Tracey Holloway (taholloway@wisc.edu), University of Wisconsin—Madison
Xiaomeng Jin (xjin@ldeo.columbia.edu), LDEO/Columbia University
Lok Lamsal (lok.lamsal@nasa.gov), NASA GSFC
George Milly (gpm2109@columbia.edu), LDEO/Columbia University
Jessica Neu (Jessica.L.Neu@jpl.nasa.gov), NASA JPL
Talat Odman (talat.odman@ce.gatech.edu), Georgia Institute of Technology
Jonathan Patz (patz@wisc.edu), University of Wisconsin—Madison
Ted Russell (ted.russell@gatech.edu), Georgia Institute of Technology
Daniel Tong (qtong@gmu.edu), George Mason University
Mark Zondlo (mzondlo@princeton.edu), Princeton University

Stakeholder Participants

Jim Boylan (James.boylan@dnr.ga.gov), GA EPD
Pat Dolwick (Dolwick.Pat@epa.gov), U.S. EPA
Mark Estes (mark.estes@tceq.texas.gov), TCEQ
Michael Geigert (Michael.Geigert@ct.gov), CT DEEP
Barron Henderson (henderson.barron@epa.gov), U.S. EPA
Kurt Kebschull (Kurt.Kebschull@ct.gov), CT DEEP
Sang-Mi Lee (slee@aqmd.gov), SCAQMD
Julie McDill (jmcdill@marama.org), MARAMA
Paul Miller (pmiller@nescaum.org), NESCAUM
Stephen Reid (sreid@baaqmd.gov), BAAQMD
Steve Soong (SSoong@baaqmd.gov), BAAQMD
Saffet Tanrikulu (STanrikulu@baaqmd.gov), BAAQMD
Di Tian (Di.Tian@dnr.ga.gov), GA EPD
Gail Tonnesen (Tonnesen.Gail@epa.gov), U.S. EPA
Luke Valin (Valin.Lukas@epa.gov), U.S. EPA
Susan Wierman (swierman@marama.org), MARAMA
Tao Zeng (Tao.Zeng@dnr.ga.gov), GA EPD

How to cite this technical guidance document:

Jin, X., A.M. Fiore, M. Geigert et al. (2018), Using satellite observed formaldehyde (HCHO) and nitrogen dioxide (NO_2) as an indicator of ozone sensitivity in a SIP, HAQAST Tech. Guid. Doc. No. 1, doi: 10.7916/D8M34C7V, available at https://doi.org/10.7916/D8M34C7V.

DISCLAIMERS

The views, opinions, and findings contained in this report are those of the authors and should not be construed as an official position, policy, or decision by any of the authors' institutions or agencies, nor may they be used for advertising or product endorsement. The guidance provided in this document was written with the intent to encourage "best practices" in using satellite data for air quality applications. Furthermore, neither the U.S. government nor any of the authors' agencies endorse or recommend any commercial products, processes, or services, including Web sites, maintained by public and/or private organizations, to which this document provides links. When users follow a link to an outside Web site, they are subject to the privacy and security policies of the owners/sponsors of the outside Web site(s). Neither the authors nor their agencies or institutions are responsible for the information collection practices of these sites. Reference to or appearance of any specific commercial products, processes, or services by trade name, trademark, manufacturer, or otherwise, in these materials does not constitute or imply its endorsement, recommendation, or favoring by the U.S. Government or any of the authors' institutions. Neither the authors nor their employers assume any liability resulting from the use of these materials.

VERSION 6-18

1. Example of CT DEEP using OMI HCHO/NO_2 in State Implementation Plans:

Although State Implementation Plans (SIPs) typically rely on observations from ground-based networks and regulatory models, satellite data is increasingly available to state agencies and can also inform and supplement state implementation plans to improve air quality. An advantage of satellite data is that it provides information for a broader area than sampled by ground-based networks. This document provides examples and guidance for using satellite products of formaldehyde (HCHO) and nitrogen dioxide (NO_2) to inform ground-level ozone sensitivity to emissions of nitrogen oxides (NO_x) versus volatile organic compounds (VOC) in state implementation plans. Analysis of changes in ozone sensitivity over periods where emission controls have been implemented can provide insights into the efficacy of those past strategies and the likely efficacy of proposed future emission control programs.

The information described below has been used in two separate Connecticut Department of Energy and Environmental Protection State Implementation Plans (SIPs):

1. See Page 20 to 21 of the *8-hour Ozone Attainment Demonstration for the Connecticut portion of the New York-Northern New Jersey-Long Island (NY-NJ-CT) Nonattainment Area Technical Support Document of Connecticut's* State Implementation Plan: http://www.ct.gov/deep/lib/deep/air/ozone/ozoneplanningefforts/SouthwestConnecticutAttainmentSIPFINAL.pdf

and

2. See page 21 of the *8-Hour Ozone Attainment Demonstration for the Greater Connecticut Nonattainment Area Technical Support Document of Connecticut's State Implementation Plan*: http://www.ct.gov/deep/lib/deep/air/ozone/ozoneplanningefforts/EnclosureAGreaterCTAD.pdf

Additional information on the two SIP revisions can be found at the following web page: http://www.ct.gov/deep/cwp/view.asp?a=2684&q=585816&deepNav_GID=1619

2. Background on HCHO/NO_2

O_3 photochemistry

O_3 formation is driven by two major classes of directly emitted precursors: nitrogen oxides (NOx) and volatile organic compounds (VOC). Depending on local relative abundances of NO_x and VOCs, O_3 formation can be mitigated by reducing NO_x emissions (NO_x-limited regime), or by reducing VOC emissions (NO_x-saturated or radical-limited or VOC-limited regime; hereafter, we refer to this regime as VOC-limited, following the common practice in the air management community). The split between NO_x-limited and VOC-limited regimes depends on which radical sink is dominant (peroxides or nitric acid (HNO_3)). When peroxides represent the dominant radical

sink, O_3 production is NO_x-limited. When HNO_3 is the dominant sink, O_3 production is VOC-limited; this regime is usually limited to urban areas. The O_3 isopleth below illustrates the nonlinear O_3-NO_x-VOC photochemistry. In the NO_x-limited regime, O_3 decreases with decreasing NO_x, but is insensitive to changes in VOCs. In the VOC-limited regime, O_3 decreases with decreasing VOCs, but increases with decreasing NO_x until a "tipping point' is reached.

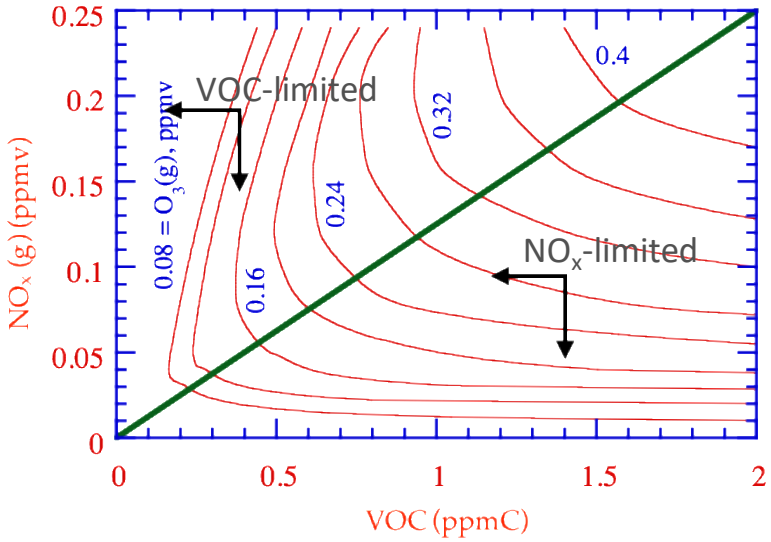

Figure 1 O_3 isopleth that illustrates the non-linear O_3-NO_x-VOC photochemistry. The red lines depict the peak O_3 mixing ratio produced by different initial mixing ratios of NO_x (y-axis) and VOC (x-axis). Figure adapted and modified from Jacobson (2002). Note this plot illustrates a general pattern. The exact dependence of O_3 on NO_x and VOC as shown in the isopleth varies with assumptions (e.g. VOC reactivity) and conditions (e.g. temperature, wind speed) used in generating the plot.

HCHO/NO_2 as an O_3 sensitivity indicator

The relationships of chemical species produced during ozone formation, such as HCHO and NO_2, reflect the processes that determine the non-linear sensitivity of O_3 to its precursor emissions of VOC and NO_x. For example, the relative ambient concentrations of HCHO and NO_2 reflect the reactivity-weighted concentrations of VOC and NO_x, respectively, and thus contain information on how O_3 will respond to changes in NO_x and VOC emissions (*Sillman*, 1995). As both HCHO and NO_2 have short lifetimes (~hours), their ratio reflects the competition between OH reaction with VOC versus NO_2 (*Tonnesen and Dennis*, 2000). Applying chemical indicator ratios requires understanding their values within the different regimes for ozone formation (i.e., NOx-limited versus VOC-limited). Identifying the values of an indicator ratio that delineate the boundaries between ozone formation regimes has typically been done with chemical transport models. An example is shown in Figure 2 below using the GEOS-Chem chemical transport model. The top panel shows the relationship between the O_3 sensitivity to an emission change and the value of the HCHO/NO_2 ratio in near-surface air. The bottom panel shows the same relationship but for the ratio of column HCHO to column NO_2; these column quantities are observable from

space by instruments aboard satellites. Both panels show a correlation between normalized surface O_3 responses to changes in NO_x and VOC emissions (y-axis; $d[O_3]/dE$) and the $HCHO/NO_2$ ratio. Figure 2 shows that higher values of $HCHO/NO_2$ ratios are typically associated with NO_x-sensitive conditions (*i.e.* $d[O_3]/dE_{NOx} > d[O_3]/dE_{VOCs}$), while lower values are typically associated with VOC-limited (*i.e.* $d[O_3]/dE_{NOx} < 0$) conditions. It also illustrates that the relationship of ozone sensitivity to emission changes with surface versus column ratios are not identical.

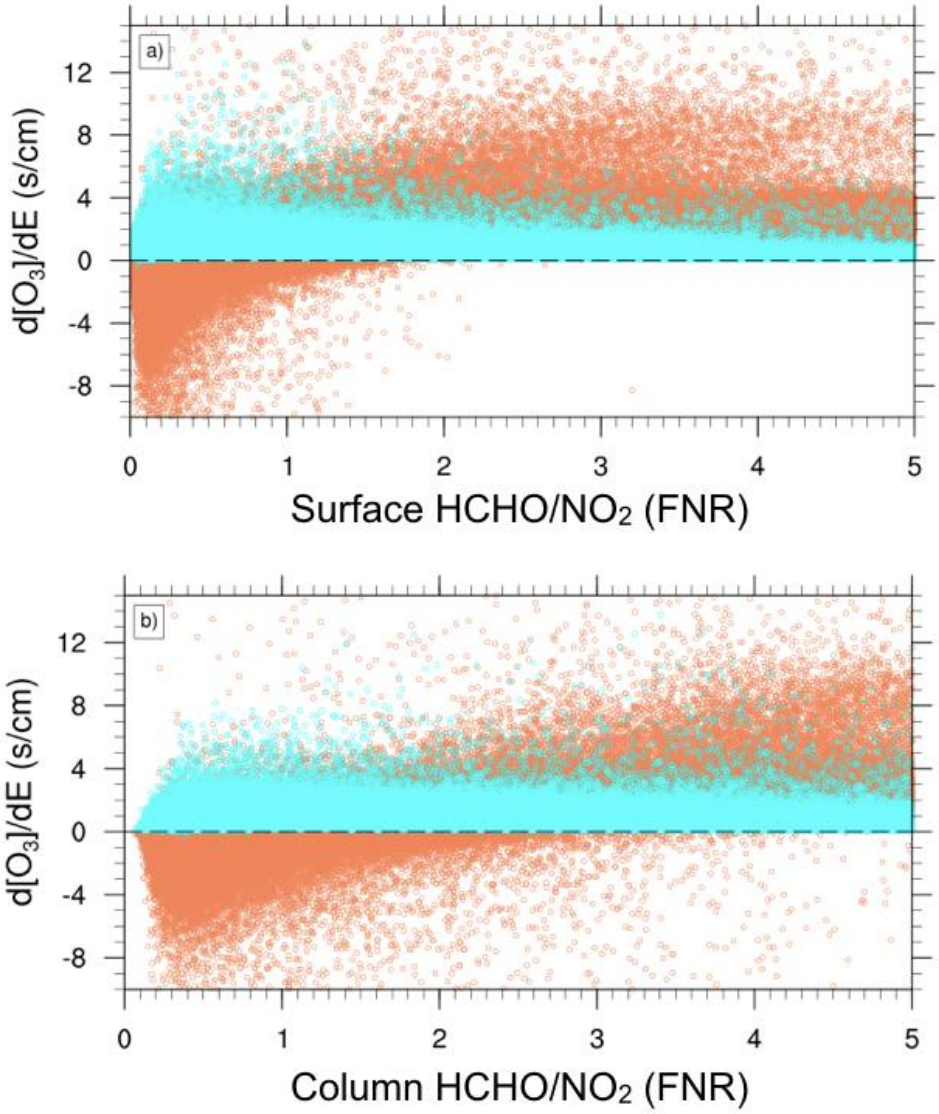

Figure 2. GEOS-Chem model (v. 9.02, http://www.geos-chem.org; 2°x2.5° horizontal resolution) estimates of the normalized O_3 sensitivity to 20% decreases in global NO_x and VOC emissions ($d[O_3]/dE_{NOx}$ in orange, $d[O_3]/dE_{VOC}$ in blue) versus the modeled (a) surface $HCHO/NO_2$ and (b) tropospheric column $HCHO/NO_2$ aggregated over the three selected regions (North America, Europe, Asia). Each point is equal to the normalized sensitivity ratios of daily one-hour averages between 1 and 2 PM from 2006 to 2012 in a single model grid cell. We only include polluted grid cells, defined as cells with average modeled tropospheric NO_2 column densities higher than 2.5×10^{15} molecules/cm^2. $[O_3]$ is

in units of molecules cm^{-3} and emissions are in units of molecules $cm^{-2}s^{-1}$, and $d[O_3]/dE$ is thus s cm^{-1}. Figure excerpted from Jin et al. [2017].

Satellite observations of HCHO and NO_2

Satellite instruments measure the total amount of HCHO and NO_2 between the surface and space, which is referred to as a column density in units of molecules cm^{-2}. For current space-based instruments, the retrieved columns often represent spatial averages over areas on the order of hundreds of square kilometers. For NO_2, we use the tropospheric column, which is equal to the total column minus the stratospheric column. *Martin et al*. [2004] first applied the indicator ratio to Global Ozone Monitoring Experiment (GOME) retrievals of HCHO and NO_2. This work has been refined and extended to Ozone Monitoring Instrument (OMI) products to characterize O_3 sensitivity over the U.S.A. [*Choi et al.*, 2012; *Duncan et al.*, 2010; *Chang et al.*, 2016; *Jin et al.*, 2017]. The finer spatial resolution of OMI (up to 13×24 km^2) better captures the urban-rural gradient of O_3 sensitivity than the coarse GOME resolution (40×320 km^2).

For more background about ozone-NO_x-VOC sensitivity:

Dr. Sanford Sillman's website "Overview: Tropospheric Ozone, Smog and Ozone-NO_x-VOC Sensitivity" (http://www-personal.umich.edu/~sillman/ozone.htm)

For more information on satellite HCHO/NO_2 for air quality management:

NASA AQAST Using Satellite Data for Air Quality Management: Chemical production of ozone (https://aqast.wisc.edu/chemical-production-of-ozone.htm)

3. Figures used in the CT SIP

Under NASA AQAST and HAQAST, collaborations were initiated between Lamont-Doherty Earth Observatory of Columbia University and CT DEEP. AQAST/HAQAST member Arlene Fiore and graduate student Xiaomeng Jin produced the figures below for CT DEEP. Taking advantage of the decade-long record of OMI HCHO and tropospheric NO_2 column observations, the figures below show the decadal changes of O_3 sensitivity over the northeast U.S.A. The days when observed ozone is highest is of most interest from an air quality policy perspective. To examine the HCHO/NO_2 ratio on these high-ozone days, we use O_3 measurements from three ground-level ozone networks interpolated to a relatively coarse 1°×1° grid (Schnell *et al.*, 2015). This interpolation will lead to smearing, and underestimate the number of days with high O_3 levels relative to that determined based on individual monitors. Figure 3 shows the average OMI HCHO/NO_2 values on the days when the gridded O_3 observations exceeded 70 ppb (defined specifically as days when the maximum daily 8-hour average (MDA8) O_3 concentration > 70 ppbv). The white area indicates either that no days exceeded 70 ppb when averaged over this particular grid cell, or that no valid OMI observations are available on the days when the gridded observations exceed 70 ppb. The figure shows more white areas in 2013 relative to 2005, due to two factors: 1) O_3 non-attainment days decreased from 2005 to 2013 (though we note that regions shown in white do contain individual monitors where the standard was exceeded); 2) OMI data coverage also decreased due to the growing row anomalies. Although data coverage from OMI is

declining as the instrument ages, HCHO and NO_2 will be retrieved from new satellite instruments, such as TROPOMI, and upcoming instruments such as TEMPO that should launch in the next few years; these will enable a continuation of this type of analysis at higher spatial (and temporal, with TEMPO) scales (see Section 4 below).

Figure 4 zooms in to the urban region of New York City to show monthly average $HCHO/NO_2$ from 2005 to 2015 in a single OMI pixel (13 x 24 km^2) located at the urban core of the city. The purple shaded regions indicate a "transition" regime where the ozone formation is shifting from being more sensitive to VOC (below the purple rectangle) to being more sensitive to NOx concentrations (i.e. NO_x-limited, the area above the purple rectangle). It reveals an increase in the column ratios of $HCHO/NO_2$ over the last decade such that in the more recent years, a couple summer (ozone season) months each year now fall in the NO_x-limited regime. Figure 4 classifies the O_3 production regime based on the constant thresholds proposed by Duncan *et al*. (2010): $HCHO/NO_2 < 1$ is VOC-limited whereas $HCHO/NO_2 > 2$ is NO_x-limited. Both Figures 3 and 4 show an increase of the $HCHO/NO_2$ values from 2005 to 2013, suggesting increasing NO_x sensitivity over northeast US.

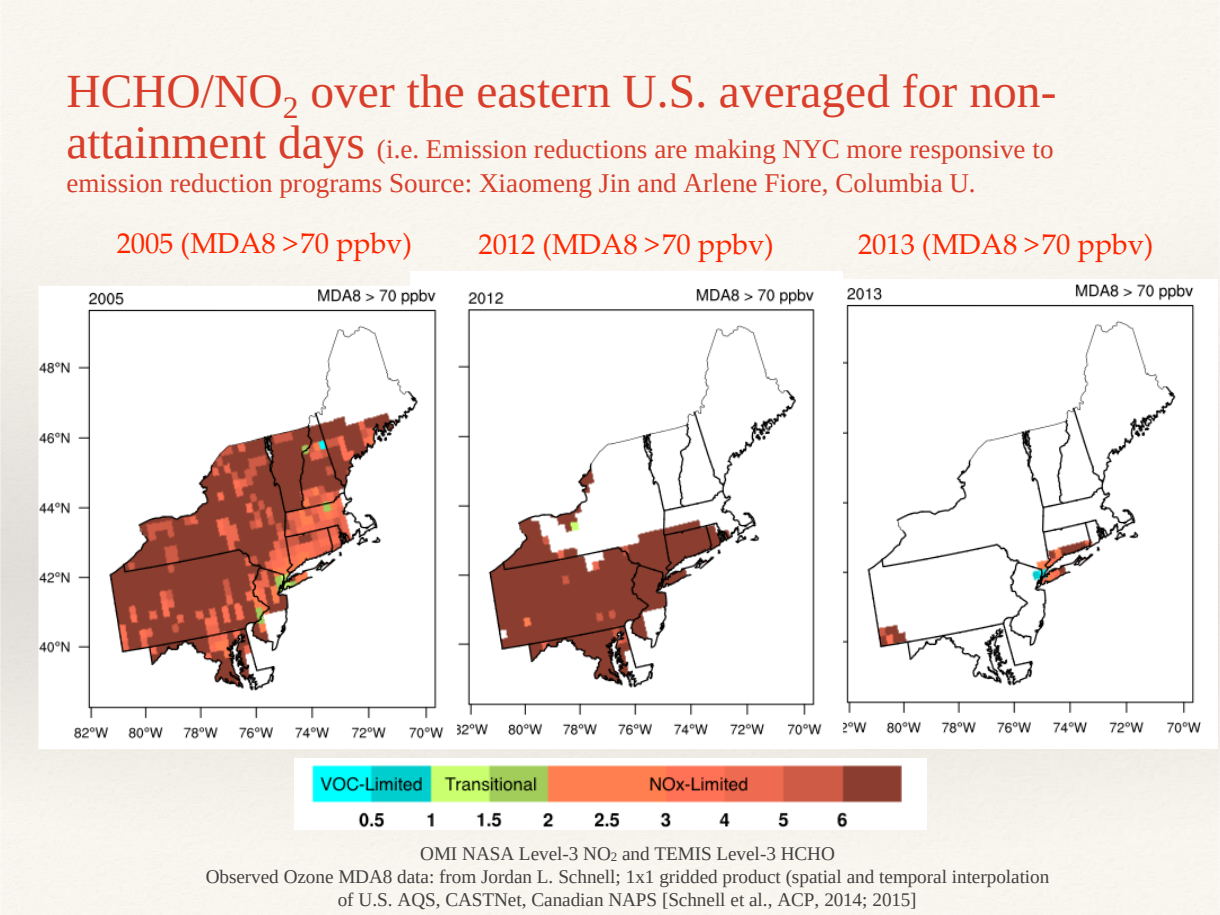

Figure 3. OMI HCHO/NO_2 over the northeastern U.S.A. averaged for MDA8 O_3 non-attainment days. O_3 non-attainment days (MDA8 O_3 > 70 ppbv) are identified from gridded O_3 products that interpolate U.S. AQS, CASTNet and Canadian NAPS to 1°×1° grid (Schnell et al., 2015). Non-attainment days are under-represented due to OMI data availability and the averaging of individual monitors to a relatively coarse spatial grid.

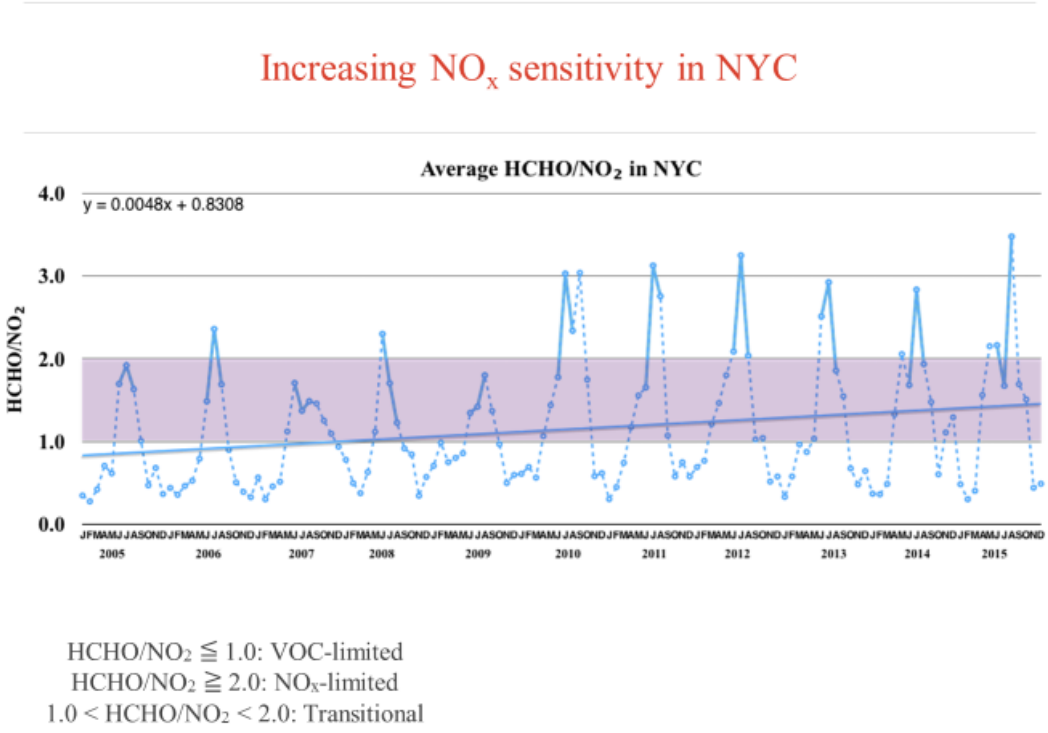

Figure 4. Time series of monthly average OMI $HCHO/NO_2$ (blue dots) for the OMI pixel encompassing New York City; solid lines indicate summer months (June, July and August). The purple shading marks the transition regime based on values reported in Duncan et al. (2010), which falls between the VOC-limited regime ($HCHO/NO_2 < 1$) and the NO_x-limited regime ($HCHO/NO_2 > 2$).

4. Re-evaluation of transition regime in Figures 3 and 4

Figure 5 is an update to Figure 4 that adjusts the values marking the boundaries of the different ozone formation regimes based on the column-to-surface relationships modeled with the GEOS-Chem chemistry-transport model. This model-based approach adjusts for the differences in the relationships between ozone responses to emission changes and the column versus surface $HCHO/NO_2$ ratios as shown in Figure 2 (Jin *et al.*, 2017). Using the constant regime threshold (1 - 2) tends to weaken the seasonal cycle and the spatial variation of the O_3-NO_x-VOC sensitivity. The maps in Figure 5 show that the northeast U.S.A. was predominantly NO_x-limited in May of 2005 and again in May of 2015. In the vicinity of New York City, however, the OMI-derived ratios indicate that the metropolitan area was VOC limited in May 2005, but shifted toward NO_x-limited by 2015 with the New York City core area shifting to a transitional regime. NO_x-limited conditions are found across northeast U.S.A. from May to September. Looking throughout the year in the time series plot shown in Figure 5, we see that the NO_x-limited regime (above the pink shaded region) occurred from June to August in NYC in 2005, and that the length of the NO_x-limited regime increased from three months in 2005 to five months in 2015. The adjustment of column-to-surface ratios leads to a seasonal variation in the $HCHO/NO_2$ values within the VOC-limited

versus NOx-limited regimes (pink shading). The average length of the NO_x-limited regime from 2005 to 2009 is 3.2 months, and increases to 4.2 months for the 2011 to 2015 period. The length of the VOC-limited regime has decreased from eight months in 2005 to five months in 2015. The five-year average length of the VOC-limited regime has decreased from 7.4 (2005 to 2009) to 6.0 months (2011 to 2015). Evidence for additional NO_x limitation is evident throughout the broader region in 2015 versus 2005 (Jin *et al.*, 2017).

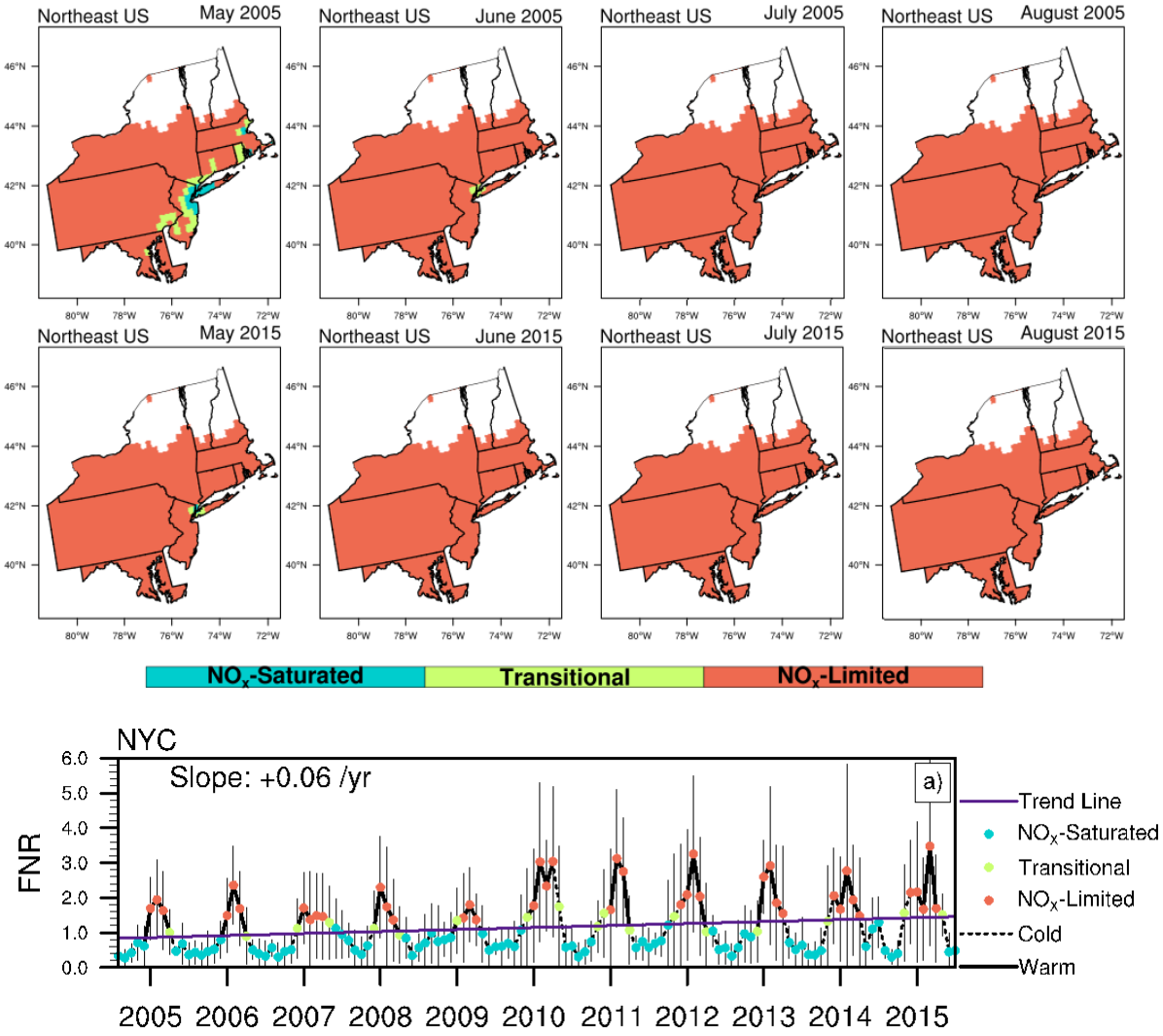

Figure 5. O_3 production regimes over the Northeast U.S.A. in May to August of 2005 and 2015 (top), and the time series of monthly OMI-derived HCHO/NO_2 (circles) along with the transition regime (pink shading) marking the boundaries between VOC-limited (below the pink band) and NO_x-limited (above the pink band) over New York City. The monthly ratios are calculated from monthly average OMI Level-3 BIRA HCHO to Level-3 NASA NO_2. Solid lines indicate the warm season (May to September) and the dashed lines indicate the cold season (October to April). Monthly transition regime threshold values are derived from the GEOS-Chem model (Figure 2) and interpolated onto the OMI grid; they are also adjusted based on the modeled column-to-surface relationships. The observed HCHO/NO_2 are monthly

average OMI Level-3 BIRA HCHO to Level-3 NASA SP NO_2 for the grid cell covering New York City. The uncertainty (error bars) is calculated from monthly standard deviation of NO_2 and HCHO using Equation (3). The purple line shows the linear regression trend. In the maps, areas with average observed tropospheric NO_2 column densities < 2.5 × 10^{15} molecules/cm^2 are masked. Details are provided in Jin et al. [2017].

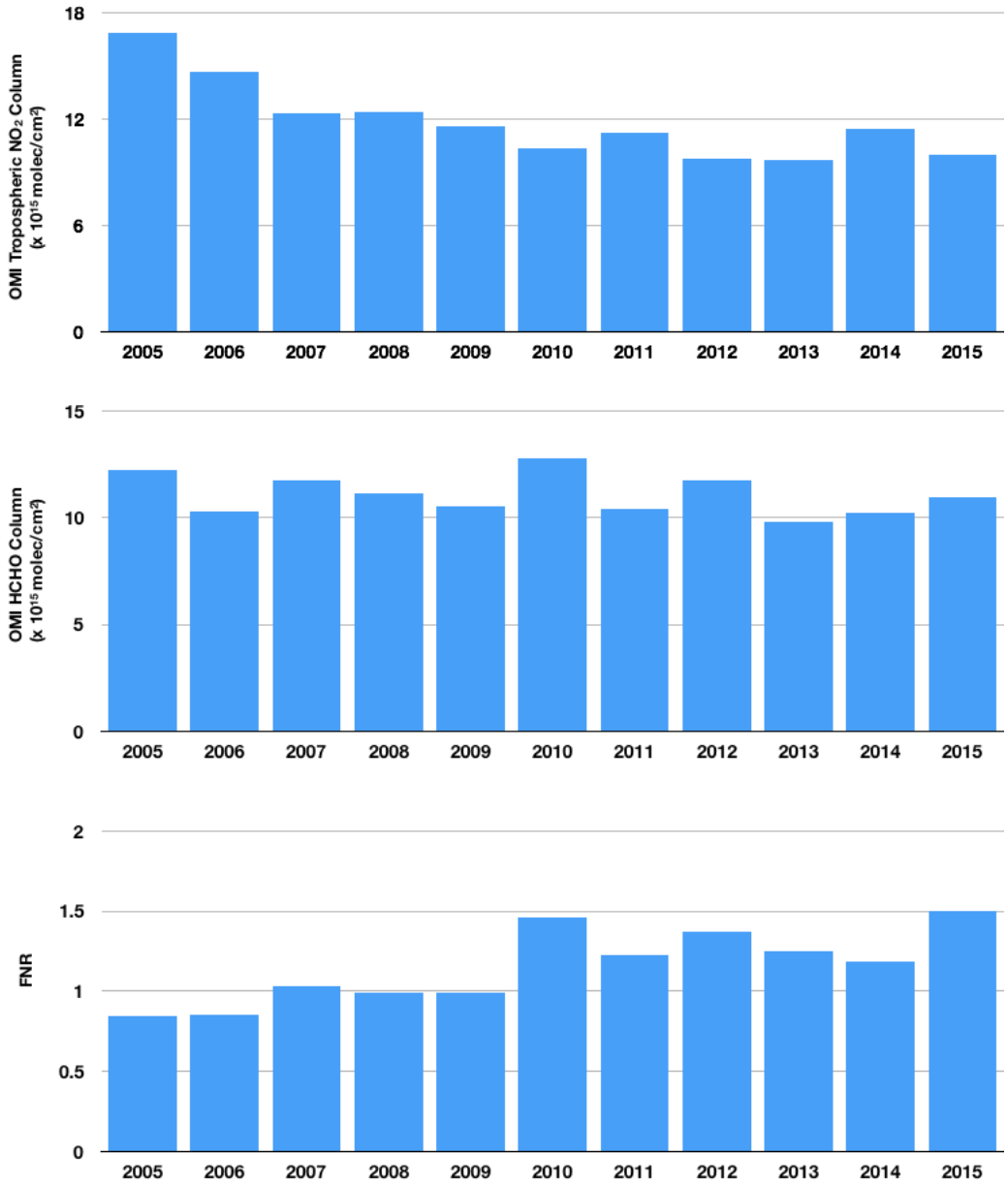

Figure 6 Bar charts of annual average tropospheric NO_2 (top), HCHO (middle) and FNR (bottom) over New York City, calculated from Level-3 monthly OMI data.

5. Method for conducting this kind of analysis from publicly available Level-3 satellite products:

A) Access OMI NO_2 data:

1) TEMIS NO_2 Data Products

NO_2 products and documentation from the European TEMIS project (KNMI, Netherlands) can be found at http://www.temis.nl/airpollution/NO2.html. TEMIS is a web-based service used to browse and download atmospheric satellite data products. These tropospheric NO_2 columns are derived from satellite observations based on slant column NO_2 retrievals with the DOAS technique, and the KNMI combined modelling/retrieval/assimilation approach. The slant columns from GOME, SCIAMACHY and GOME-2 observations are derived by BIRA-IASB, the slant columns from OMI by KNMI/NASA (Boersma *et al.*, 2011).

On the TEMIS products web page, there is a link for monthly regional NO_2 products: http://www.temis.nl/airpollution/NO2col/NO2regioomimonth_v2.php. Since the ozone sensitivity analysis uses NO_2 monthly means, it is useful to get an image of the data that is being analyzed (e.g. Figure 7).

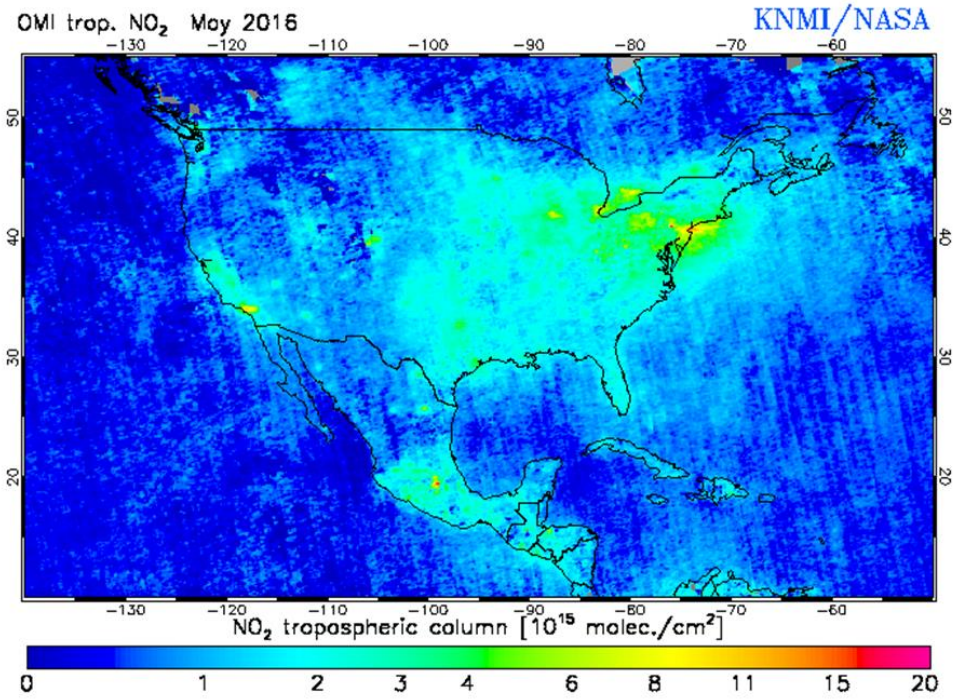

Figure 7 A sample image from the TEMIS website showing monthly average OMI NO_2 over North America in May 2016..

The TEMIS web site provides downloads for a KML file, and zip-ed ASCII data files in TOMS and ESRI grid formats. No registration is needed to download the data. The files are compressed in .tar format. A Mac system can automatically unpack the files after downloading the data. For Windows users, you may need something like this open source 'unpacking' utility

from http://www.7-zip.org/ . You can use 7-Zip on any computer, including a computer in a commercial organization. You don't need to register or pay for 7-Zip. After downloading and installing this application, you can use it to unpack any compressed file right from the Windows file manager.

2) NASA EARTHDATA NO_2 Data Products

The NASA Earthdata site is another repository for OMI NO_2 satellite data. Unlike TEMIS, the monthly mean data is not available from the NASA EARTHDATA Level 3 data downloads for NO_2. Daily data can be downloaded and are in he5 (HDF) format. Using this service will require you to register free with the Earthdata web site. For more information about OMI NO_2 data, see the technical guidance for OMI NO_2 written by Bryan Duncan at NASA Goddard. The he5 files can be then plotted using a viewer such as this offered by NASA: https://www.giss.nasa.gov/tools/panoply/. Panoply plots geo-referenced and other arrays from netCDF, HDF, GRIB, and other datasets.

B) Using Panoply to view/extract NO_2 data

1) TEMIS Data:

As mentioned before, the TEMIS web site provides downloads for monthly average KML files, and zipped ASCII data files in TOMS and ESRI grid formats. These are not readily viewable in Panoply, but the ASCII data file in TOMS format can be viewed in a spreadsheet or any text file editor (e.g. ultraedit, vi). If one is only interested in a specific location, the monthly average column density can be found from the text file by locating the latitude and longitude. Detailed information on reading the ASCII file can be found here. If one is interested in making a map of HCHO/NO_2, it is recommended to convert the ascii file to a file format that has geographic information (e.g. netcdf, geotiff). Once converted to NetCDF, the data can then be displayed in Panoply. Figure 8 (a) is a screenshot created with Panoply that shows the monthly average tropospheric NO_2 column density (in units of 10^{15} molecules/cm^2) over the USA in May 2016. The KML file can be saved and viewed in Google Earth. Figure 8 (b) is a map that was downloaded as a KML for May, 2016. If the ESRI ArcGIS products are at your disposal, then the ESRI Gridded formatted data can be plotted. This data needs to be georeferenced within ArcCatalog before it can be plotted. Figure 8 (c) is what the OMI May 2016 looks like in ArcMAP after the data intervals have been manually selected and the colors changed. For comparison, Figure 8 (d) the GOME-2 ESRI gridded data for the same period and plotted in ArcMAP (below). GOME-2 satellite pixels have a coarser resolution than OMI, which is apparent in the image and the NO_2 concentrations tend to be higher.

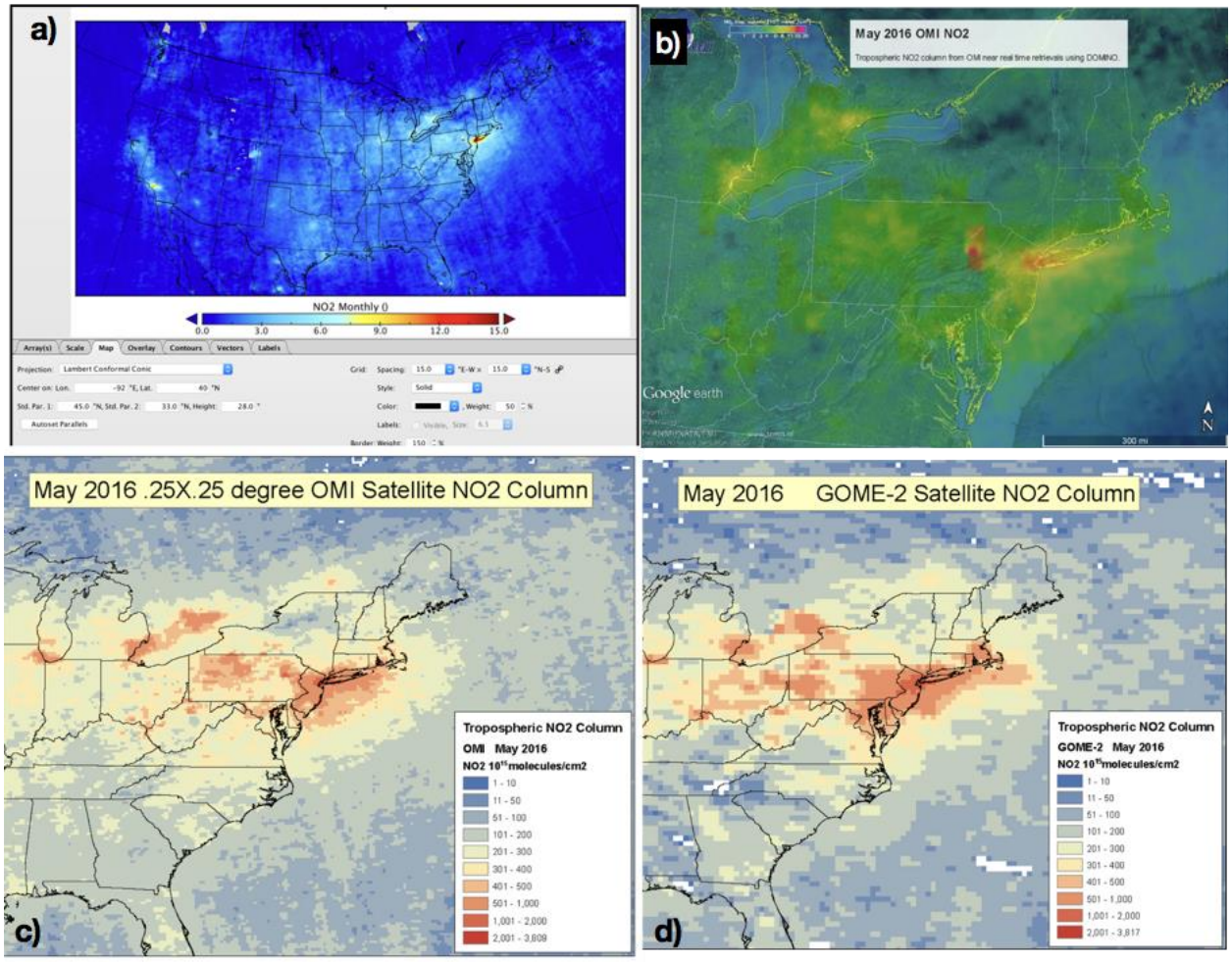

Figure 8. Images of monthly average tropospheric NO_2 column density in May 2016 made from: a) Panoply; b) Google Earth; c)ArcMAP using OMI data; d) ArcMAP using GOME-2 data.

2) NASA OMI NO_2 Product:

The Earthdata web site provides downloads in the HDF (.he5) format, which can be read by various tools. Figure 9 is a screen shot of the menu tree in Panoply for plotting the May 20, 2016 cloud screened tropospheric NO_2 column density. It is important that you choose the GEO2D file type for plotting, otherwise there will be no georeference for the map that is produced. The following map was easily produced after changing the map projection and adjusting the color scale ranges. Panoply also allows you to covert the gridded data to .csv file, which is readily viewed in a spreadsheet (Figure 9).

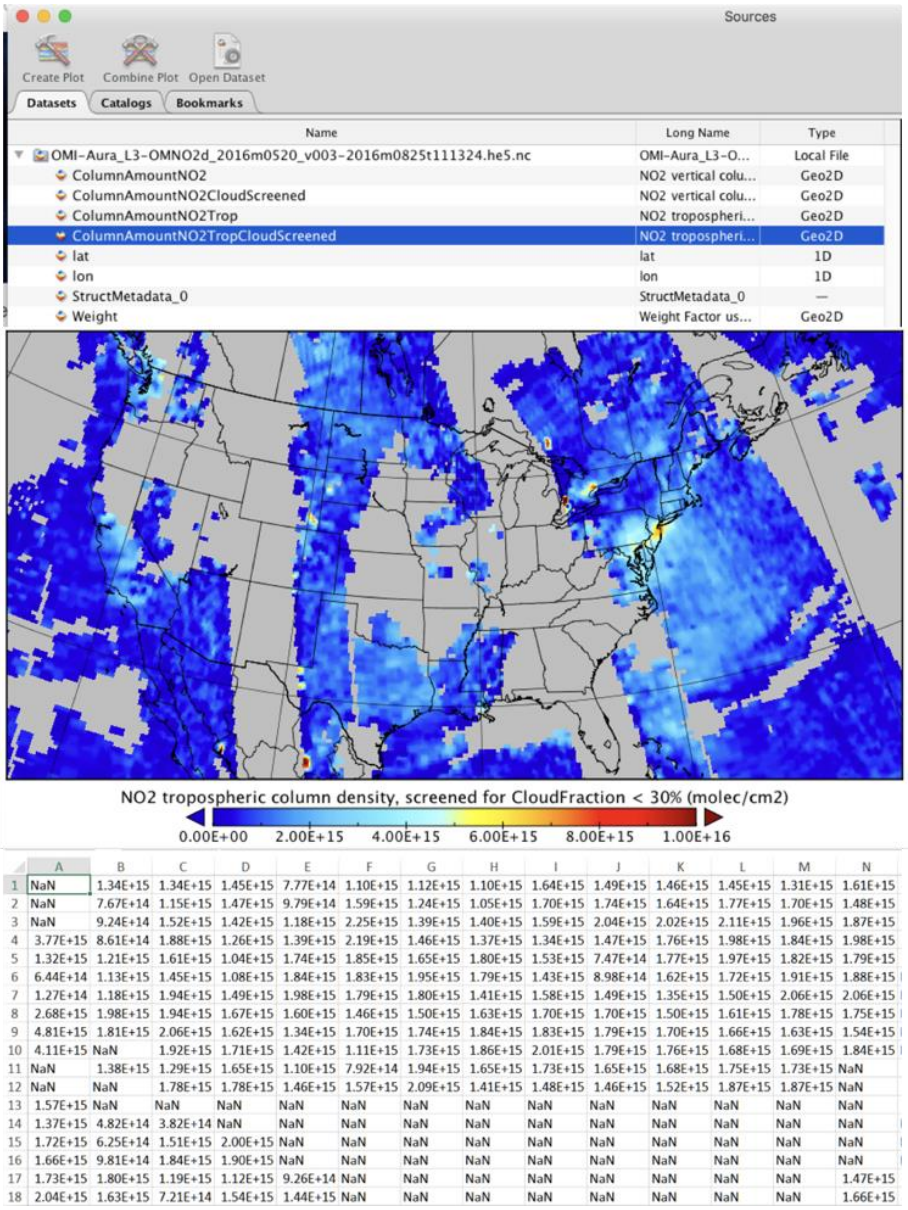

	A	B	C	D	E	F	G	H	I	J	K	L	M	N
1	NaN	1.34E+15	1.34E+15	1.45E+15	7.77E+14	1.10E+15	1.12E+15	1.10E+15	1.64E+15	1.49E+15	1.46E+15	1.45E+15	1.31E+15	1.61E+15
2	NaN	7.67E+14	1.15E+15	1.47E+15	9.79E+14	1.59E+15	1.24E+15	1.05E+15	1.70E+15	1.74E+15	1.64E+15	1.77E+15	1.70E+15	1.48E+15
3	NaN	9.24E+14	1.52E+15	1.42E+15	1.18E+15	2.25E+15	1.39E+15	1.40E+15	1.59E+15	2.04E+15	2.02E+15	2.11E+15	1.96E+15	1.87E+15
4	3.77E+15	8.61E+14	1.88E+15	1.26E+15	1.39E+15	2.19E+15	1.46E+15	1.37E+15	1.34E+15	1.47E+15	1.76E+15	1.98E+15	1.84E+15	1.98E+15
5	1.32E+15	1.21E+15	1.61E+15	1.04E+15	1.74E+15	1.85E+15	1.65E+15	1.80E+15	1.53E+15	7.47E+14	1.77E+15	1.97E+15	1.82E+15	1.79E+15
6	6.44E+14	1.13E+15	1.45E+15	1.08E+15	1.84E+15	1.83E+15	1.95E+15	1.79E+15	1.43E+15	8.98E+14	1.62E+15	1.72E+15	1.91E+15	1.88E+15
7	1.27E+14	1.18E+15	1.94E+15	1.49E+15	1.98E+15	1.79E+15	1.80E+15	1.41E+15	1.58E+15	1.49E+15	1.35E+15	1.50E+15	2.06E+15	2.06E+15
8	2.68E+15	1.98E+15	1.94E+15	1.67E+15	1.60E+15	1.46E+15	1.50E+15	1.63E+15	1.70E+15	1.70E+15	1.50E+15	1.61E+15	1.78E+15	1.75E+15
9	4.81E+15	1.81E+15	2.06E+15	1.62E+15	1.34E+15	1.70E+15	1.74E+15	1.84E+15	1.83E+15	1.79E+15	1.70E+15	1.66E+15	1.63E+15	1.54E+15
10	4.11E+15	NaN	1.92E+15	1.71E+15	1.42E+15	1.11E+15	1.73E+15	1.86E+15	2.01E+15	1.79E+15	1.76E+15	1.68E+15	1.69E+15	1.84E+15
11	NaN	1.38E+15	1.29E+15	1.65E+15	1.10E+15	7.92E+14	1.94E+15	1.65E+15	1.73E+15	1.65E+15	1.68E+15	1.75E+15	1.73E+15	NaN
12	NaN	NaN	1.78E+15	1.78E+15	1.46E+15	1.57E+15	2.09E+15	1.41E+15	1.48E+15	1.46E+15	1.52E+15	1.87E+15	1.87E+15	NaN
13	1.57E+15	NaN	NaN	NaN	NaN	NaN	NaN	NaN	NaN	NaN	NaN	NaN	NaN	NaN
14	1.37E+15	4.82E+14	3.82E+14	NaN	NaN	NaN	NaN	NaN	NaN	NaN	NaN	NaN	NaN	NaN
15	1.72E+15	6.25E+14	1.51E+15	2.00E+15	NaN	NaN	NaN	NaN	NaN	NaN	NaN	NaN	NaN	NaN
16	1.66E+15	9.81E+14	1.84E+15	1.90E+15	NaN	NaN	NaN	NaN	NaN	NaN	NaN	NaN	NaN	NaN
17	1.73E+15	1.80E+15	1.19E+15	1.12E+15	9.26E+14	NaN	NaN	NaN	NaN	NaN	NaN	NaN	NaN	1.47E+15
18	2.04E+15	1.63E+15	7.21E+14	1.54E+15	1.44E+15	NaN	NaN	NaN	NaN	NaN	NaN	NaN	NaN	1.66E+15

Figure 9. Daily OMI observed tropospheric NO_2 column plotted in Panoply.

C) Accessing OMI HCHO Data

1) TEMIS HCHO Data Products

HCHO products are available at the European TEMIS project (KNMI, Netherlands). This web site produces daily, monthly and yearly mean images and ASCII gridded data files for download. Level 2 data files are available on request (HDF5 format), while level 3 daily and monthly gridded vertical columns (ASCII format) are provided on TEMIS. The monthly global mean image for HCHO for May 2016 is shown in Figure 10.

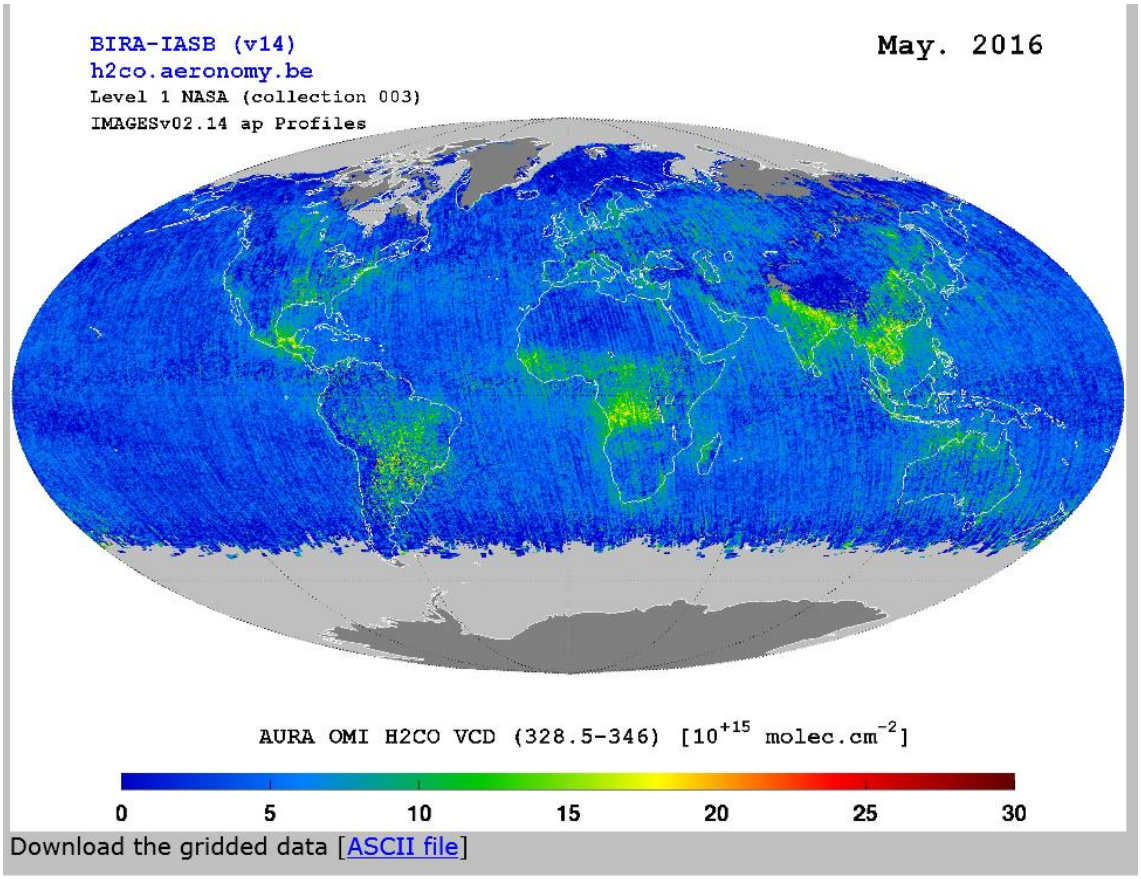

Figure 10. An example image of OMI monthly average HCHO column density in May 2016 available from TMEIS website.

Similar to NO_2 data, the ASCII file can be converted to NetCDF to include geographic information. The following figure is a screen shot created with panoply that shows the monthly average HCHO column density (in units of 10^{15} molecules/cm^2) over the eastern USA in May 2016.

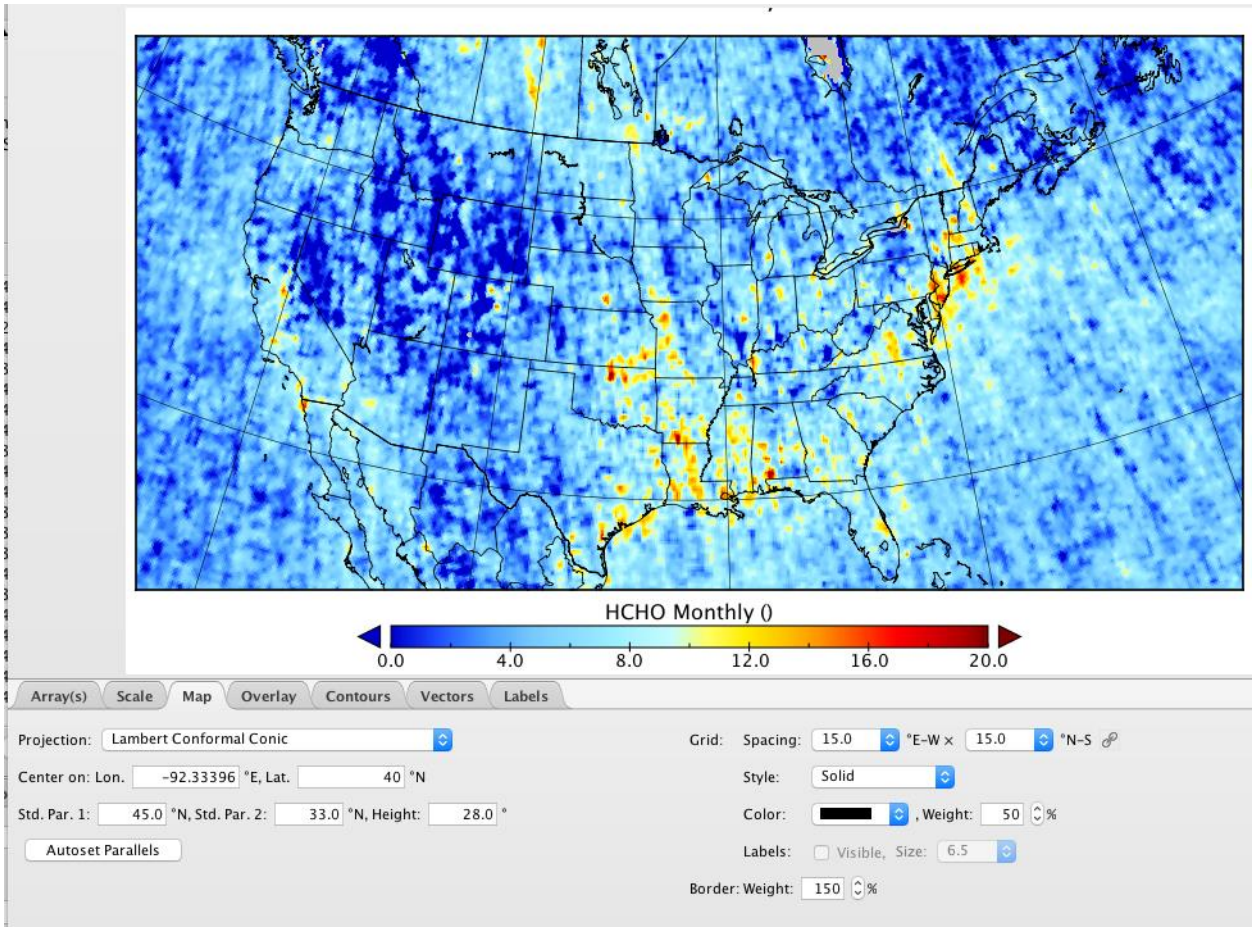

Figure 11. Images of monthly average OMI HCHO column density in May 2016 made from Panoply. ***This map illustrates the raw data****, which has not been filtered for noise because panoply does not offer a function to allow this kind of filtering.* ***V****alues in many regions fall below the detection limit (where HCHO column density < 1.5 × 10^{15} molecules/cm^2). HCHO is a particularly challenging retrieval and thus noisy. Increasing the temporal and/or spatial averaging can reduce this noise.*

2) NASA HCHO Data Products

The NASA EARTHDATA site also has access to HCHO data. Only Level 2 and Level 2G HCHO data are available from NASA.

D) Quality Assurance

For advanced uses (e.g. comparison with models), Level-2 products, which contain column density and additional geophysical parameters (e.g. scattering weight, solar zenith angle) at ground-pixel resolution along the instrument track, are recommended. (For more information on satellite product levels, see https://science.nasa.gov/earth-science/earth-science-data/data-

processing-levels-for-eosdis-data-products). In this case, it is important to apply quality control flags. When using Level-2 products, it is recommended to seek guidance from the developers to ensure appropriate screening and quality control measures are applied.

Level-3 satellite products are produced from Level-2 products by using best pixel data over each grid cell, so these products already incorporate the appropriate quality control measures.

We recommend consulting this reference before using satellite data for air quality applications: Duncan et al. (2014), titled "Satellite data of atmospheric pollution for U.S. air quality applications: Examples of applications, summary of data end-user resources, answers to FAQs, and common mistakes to avoid."

E) Calculate the ratio:

We first note that in cases where both spatial and temporal averaging of the satellite HCHO and NO_2 products must be done, the order of averaging matters to ensure an accurate calculation of the indicator ratio. This arises mainly from uneven sampling caused by large amounts of missing values. Our recommendation is to conduct any temporal averaging first before spatially averaging. This approach is most consistent with the publicly available NASA Level-3 monthly NO_2 products.

The indicator ratio is calculated by taking the ratio of satellite-observed HCHO column to tropospheric NO_2 column. To reduce the random noise of satellite data, we recommend first taking at least seven-day (or preferably monthly) averages, and then calculating the ratio of the seven-day (or monthly) average HCHO to NO_2 [*Duncan et al*., 2014]. Negative columns may be present in the NO_2 or HCHO datasets, which occur as a result of minimizing residuals during the spectral fitting below the satellite detection limits. We recommend including negative values when calculating averages, otherwise the columns may be overestimated. As described below, we only calculate ratios for areas where annual average tropospheric NO_2 columns exceed 2.5×10^{15} molecules cm^{-2}.

Panoply can perform mathematic operations on two data sets; for example, you can calculate the HCHO:NO_2 (FNR) ratio directly within panoply. To calculate a monthly FNR, one needs the level 3 quality assured gridded data, which have to be produced for Panoply. To illustrate how to use monthly gridded data to calculate the ratio, below we show an example using the monthly average OMI HCHO and NO_2 data available from TEMIS website.

To calculate the ratio of HCHO to NO_2, use the mathematical operations available from Panoply (Figure 12). The resulting ratio is shown in Figure 12. The green areas are generally VOC-limited, and the red areas are generally NO_x-limited. Note that monthly average data include some negative values, mostly because the tropospheric NO_2 level over that particular grid cell is below the detection limit. These negative values need to be filtered out, but Panoply does not provide this functionality. Note satellite data may show noise over areas where NO_2

is very low. We often mask out the areas with low NO_2 columns (e.g. annual average tropospheric NO_2 column < 2.5×10^{15} molecules/cm^2) when plotting maps, but Panoply does not have this masking function. Please see the following section, which describes our approach to classify the ozone production regime.

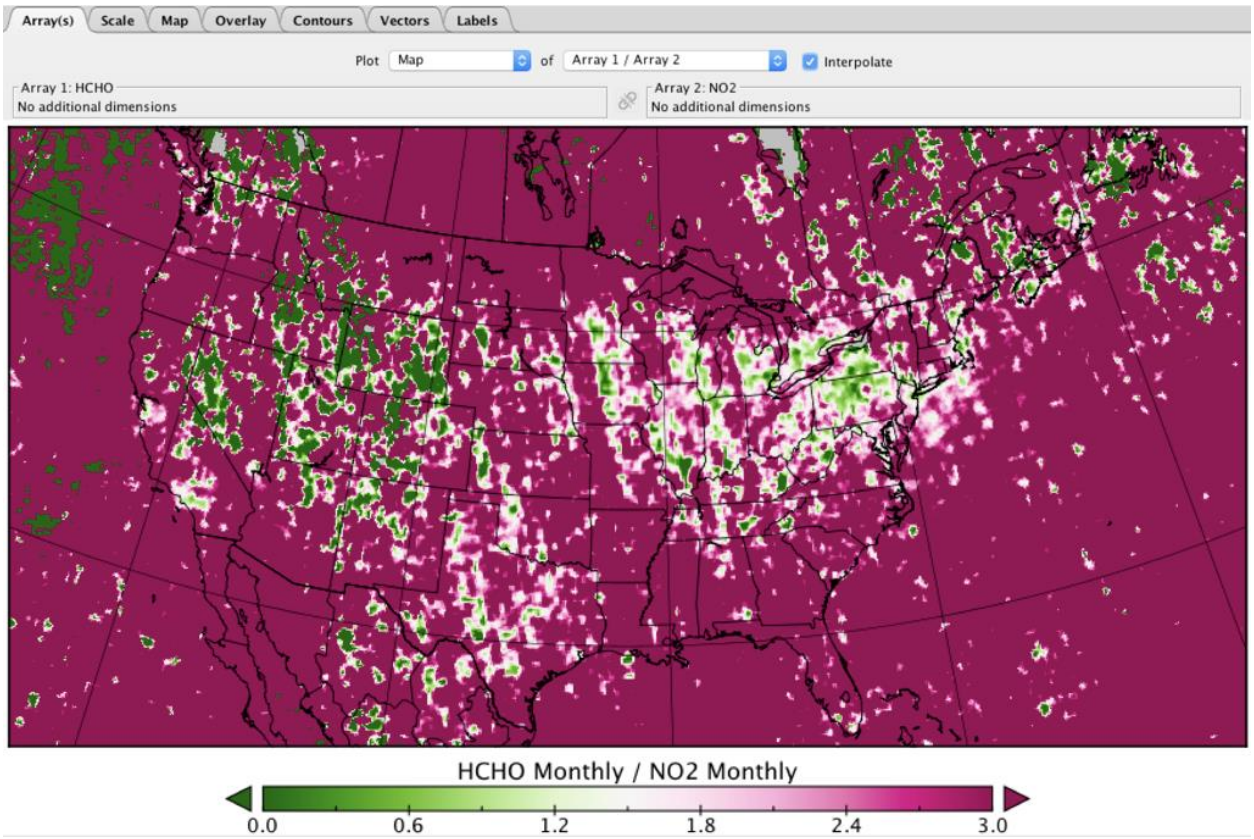

Figure 12. Monthly average FNR in May 2016 over North America made from Panoply. ***This map illustrates the raw data****, which has not been filtered for noise because panoply does not offer a function to allow this kind of filtering.* ***V****alues in many regions fall below the detection limit (where HCHO column density < 1.5×10^{15} molecules/cm^2). HCHO is a particularly challenging retrieval and thus noisy. Increasing the temporal and/or spatial averaging can reduce this noise.*

F) Infer O_3 sensitivity:

An important step for the use of satellite-derived HCHO/NO_2 is to identify the threshold values marking the transition between chemical production regimes. *Duncan et al.* [2010] estimated that the regime transition from VOC-limited to NO_x-limited chemistry occurs across a column FNR range of 1 – 2. The O_3 production regime shown in Figures 3 and 4 is based on these regime threshold values. However, Jin et al. (2017) suggest that extending the surface-based predictor to a column-based quantity requires accounting for differences in the HCHO and NO_2 vertical profiles. The regime threshold values used in this document are based

on GEOS-Chem modeled column-to-surface relationships between column and surface HCHO/NO_2. The resulting regime threshold values vary with space and time. For example, threshold values may differ in summer versus winter, and in urban versus rural or remote areas. Please contact Arlene Fiore (amfiore@ldeo.columbia.edu) and Xiaomeng Jin (xjin@ldeo.columbia.edu) to request files with the regime threshold values derived from GEOS-Chem.

G) Other satellite products available for estimating HCHO/NO_2:

Similar analysis can be applied to satellite data from other instruments that retrieve column HCHO and NO_2. These include GOME (Global Ozone Monitoring Experiment), GOME-2 and SCIAMACHY (Envisat SCanning Imaging Absorption spectroMeter for Atmospheric CHartographY). The following table shows the relevant information for these satellite instruments. In the near future, the ESA Tropospheric Ozone Monitoring Instrument (TROPOMI), which is a follow-on instrument to OMI but with finer horizontal resolution will launch soon on the polar-orbiting Sentinel-5 Precursor satellite and is targeting a 7x7 km^2 pixel size. The NASA Tropospheric Emissions: Monitoring of Pollution (TEMPO) is planned to launch in the next few years. TEMPO will be in geostationary orbit over North America. The advantage of geostationary orbit is that the instrument will stare at North America all the time, collecting hourly data throughout the day at high spatial resolution (pixel size of 2.1x4.7 km^2) [*Duncan et al*., 2014].

For more information on GOME and SCIAMACHY NO_2 products, see:
http://www.temis.nl/airpollution/NO_2.html
For more information on GOME and SCIAMACHY HCHO products, see:
http://h2co.aeronomie.be

*Table **1.** Information on the satellite instruments that measure tropospheric NO_2 and HCHO column density.*

Instrument	**Platform**	**Time Period**	**Nadir Resolution (km^2)**	**Overpass time (Local Time)**	**Global coverage (days)**
GOME	ERS-2	1995–2003	320 × 40	10:30 AM	3
SCIAMACHY	ENVISAT	2002–	60 × 30	10:00 AM	6
OMI	Aura	2004–	24 × 13	1:45 PM	1
GOME-2	MetOp	2006–	80 × 40	9:30 AM	1
TROPOMI	Sentinel-5	2017-	7 × 3.5	1:30 PM	1
TEMPO (future)	??	??	~2.2 x 4.7	~Hourly resolution	only North America

6. Questions?

Please contact Arlene Fiore (amfiore@ldeo.columbia.edu) and Xiaomeng Jin (xjin@ldeo.columbia.edu)

Or other HAQAST members: Bryan Duncan at NASA Goddard (bryan.n.duncan@nasa.gov)

Please find relevant data processing scripts at:

http://blog.ldeo.columbia.edu/atmoschem/datasets/

For general questions on the usage of satellite data in air quality, please refer to the review paper by Duncan et al. (2014), titled, Satellite data of atmospheric pollution for U.S. air quality applications: Examples of applications, summary of data end-user resources, answers to FAQs, and common mistakes to avoid.

7. Limitations to keep in mind:

1) The indicator ratios are associated with the instantaneous production rate of O_3, not necessarily the ambient O_3 mixing ratio. Ambient O_3 is the result of photochemistry and transport over several hours, and ambient VOC and NO_x can vary greatly over time and through the upwind region in which O_3 was produced.
2) The current spatial resolution of Level-3 OMI data is 0.25 °× 0.25 ° (~ 25 km resolution), which may be too coarse to reveal VOC-limited chemistry over urban cores.
3) OMI satellite data may not depict the short-term variability of O_3 chemistry well. While OMI data have near daily global coverage, satellite instruments cannot retrieve HCHO and NO_2 in the presence of cloud and snow. The random noise of a single retrieval is large. Therefore, the use of OMI HCHO/NO_2 for a single day is not recommended.
4) The OMI overpass time is around 1:45 PM (Local Time), when NO_2 is lowest during a day. OMI HCHO/NO_2 is thus higher than the daily average, meaning that OMI observation should show larger spatial extents of the NO_x-limited regime than may occur at other times of day.
5) The split of NO_x-limited and VOC-limited regime is subject to uncertainties. The regime threshold values discussed above are based on a global chemical transport model at 2 × 2.5° resolution. Evaluation using *in situ* observations is needed to assess the universality of these model-derived values for the transitions between O_3 production regimes.

8. References:

Boersma, K. F., Eskes, H. J., Dirksen, R. J., van der A, R. J., Veefkind, J. P., Stammes, P., Huijnen, V., Kleipool, Q. L., Sneep, M., Claas, J., Leitão, J., Richter, A., Zhou, Y., and Brunner, D.: An improved tropospheric NO_2 column retrieval algorithm for the Ozone Monitoring Instrument (2011), *Atmos. Meas. Tech.*, 4, 1905-1928, https://doi.org/10.5194/amt-4-1905-2011.

Chang, C.-Y., E. Faust, X. Hou, P. Lee, H. C. Kim, B. C. Hedquist, and K.-J. Liao (2016), Investigating ambient ozone formation regimes in neighboring cities of shale plays in the Northeast United States

using photochemical modeling and satellite retrievals, *Atmospheric Environment*, 1–44, doi:10.1016/j.atmosenv.2016.06.058.

Duncan, B. N. et al. (2010), Application of OMI observations to a space-based indicator of NOx and VOC controls on surface ozone formation, *Atmospheric Environment*, *44*(18), 2213–2223, doi:10.1016/j.atmosenv.2010.03.010.

Duncan, B. N. et al. (2014), Satellite data of atmospheric pollution for U.S. air quality applications: Examples of applications, summary of data end-user resources, answers to FAQs, and common mistakes to avoid, *Atmospheric Environment*, *94*, 647–662, doi:10.1016/j.atmosenv.2014.05.061.

Jin, X. et al. (2017), Evaluating a Space-Based Indicator of Surface Ozone-NO_x-VOC Sensitivity Over Midlatitude Source Regions and Application to Decadal Trends, *J. Geophys. Res. Atmos.*, *110*(9), D11303–23, doi:10.1002/2017JD026720.

Martin, R. V., A. M. Fiore, and A. V. Donkelaar (2004), Space-based diagnosis of surface ozone sensitivity to anthropogenic emissions, *Geophys. Res. Lett.*, *31*(6), L06120, doi:10.1029/2004GL019416.

Schnell, J. L. et al. (2015), Use of North American and European air quality networks to evaluate global chemistry–climate modeling of surface ozone, *Atmos. Chem. Phys.*, *15*(18), 10581–10596, doi:10.5194/acp-15-10581-2015.

Sillman, S. (1995), The Use of Noy, H2o2, and Hno3 as Indicators for Ozone-Nox-Hydrocarbon Sensitivity in Urban Locations, *J. Geophys. Res. Atmos.*, *100*(D7), 14175–14188, doi:10.1029/94JD02953.

Tonnesen, G. S., and R. L. Dennis (2000), Analysis of radical propagation efficiency to assess ozone sensitivity to hydrocarbons and NO_x: 2. Long-lived species as indicators of ozone concentration sensitivity, *Journal of Geophysical Research: Atmospheres (1984–2012)*, *105*(D7), 9227–9241, doi:10.1029/1999JD900372.